ONLINE SUPPLEMENTAL INFORMATION

p38 MITOGEN-ACTIVATED PROTEIN KINASE REGULATES CHAMBER SPECIFIC PERINATAL GROWTH IN HEART

Tomohiro Yokota[1], Jin Li[1], Jijun Huang[1], Zhaojun Xiong[1, 7], Qing Zhang[2], Tracey Chan[2], Yichen Ding[3, 4], Christoph Rau[1], Kevin Sung[3], Shuxun Ren[1], Rajan Kulkarni[3, 5], Tzung Hsiai[3, 4], Xinshu Xiao[2], Marlin Touma[8], Susumu Minamisawa[6] and Yibin Wang[1, *]

1) Departments of Anesthesiology, Physiology and Medicine, Cardiovascular Research Laboratories, David Geffen School of Medicine, University of California, at Los Angeles Los Angeles, CA 90095, USA
2) Integrative Biology and Physiology, David Geffen School of Medicine, University of California at Los Angeles, Los Angeles, CA, USA.
3) Department of Bioengineering, School of Engineering and Applied Sciences, University of California, Los Angeles, CA 90095, USA
4) Division of Cardiology, Department of Medicine, David Geffen School of Medicine at UCLA, Los Angeles, CA 90095, USA
5) Division of Dermatology, Department of Medicine, David Geffen School of Medicine at UCLA, Los Angeles, CA 90095, USA
6) Department of Cell Physiology, Jikei University, Tokyo, Japan.
7) Department of Cardiology, The 3rd Affiliated Hospital of Sun Yat-sen University, Guangzhou, China
8) Department of Pediatrics, David Geffen School of Medicine at UCLA, Los Angeles, CA 90095.

ONLINE SUPPLEMENTAL FIGURES

FIGURE LEGEND:

Figure S1. RV-specific abnormality in the cardiac-specific p38 α/β MAP kinases knockout mouse heart. (A) Representative genomic DNA PCR showing the floxed alleles of *mapk14* (p38α) and *mapk11* (p38β). **(B)** Representative immunoblot of p38 protein in the ventricular tissues from the Control and p38cdKO heart. (**C**). H&E stained histological images of one-month old control and p38cdKO ventricles. (**D-E**) Representative images of Masson trichrome stained tissue sections from the P7 **(D)** and the one-month old **(E)** Control and p38cdKO hearts. (**F**) Schematic illustration of the direction of M-mode echocardiogram conducted in this study to obtain the RV parameters as well as LV parameters. RVW, right ventricle wall thickness, RVID, right ventricle inner diameter, LVW, left ventricle wall thickness, LVID, left ventricle inner diameter. (**G**). Representative 2-D echocardiogram of image from 1-month old Control and p38-cdKO mice**.**

Figure S2. YAP and GSK3 signaling pathways in the p38cdKO RV. (**A-C**) Representative immunoblot (**A**) and quantification for YAP (**B**) and Gsk3β (**C**) in P3 RV tissue from the Control and the p38cdKO hearts as indicated. (n=3, mean ± SEM) (**D**) Representative immunohistochemical staining of Wee1 and Tropomyosin (TPM) in the left (LV) and the right (RV) ventricle of the P7 Control and p38-cdKO hearts.

Figure S3. Immunohistochemistry of myocyte apoptotic and hypertrophy in neonatal hearts. **(A-B)** Representative images of TUNEL staining in the LV (A) and the RV (B) from P3 mice. (**C-F**) Representative images of WGA staining of the Control or the p38 cdKO RV from P1 (**C, E**) and 1 month (**D, F**) old age. **(G-N)** Representative images of WGA staining in the control or the p38 cdKO LV at E19.5 (**G, K**), P1 (**H, L**), P3 (**I, M**), and 1 month (**J, N)** of age. Scale bar indicates 40 μm.

Figure S4, Gene expression profile in LV. **(A-B)** GO classification of up-regulated genes in LV of p38cdKO heart at P1 (**A**) and P3 (**B**). **(C-D)** GO classification of down-regulated genes LV of p38cdKO heart at P1 (**C**) and P3 (**D**) stages. (**E**) Heatmaps from

all differentially express genes between p38cdKO and Control in each ventricle at P1. (**F**) Reduced Dusp26 expression by siDusp26 mediated silencing in NRVM, (n=3, mean ± SEM).). For all panels, p value (vs. siNC, Control vs. cdKO) ** $p<0.01$, *$p<0.05$. (LV vs. RV) # $p<0.05$.

Figure S5. Wg-rVista analysis on differentially expressed genes in P1 and P3 LV. Top bracket includes transcription factors over-represented for all upregulated genes and bottom bracket includes transcription factors over-represented for all down-regulated genes.

Figure S6. Expression of ER stress markers. (A) RV and **(B)** LV expression ATF6, Bip, Grp94, and CHOP in P3 mouse hearts. **(C)** Levels of cytosolic sXbp1 mRNA in LV vs. RV. P value (control vs. cdKO) * $p<0.05$. (n=3, mean ± SEM). (**D**). Effect of IRE1α expression on cardiomyocyte proliferation based on Ki67 and Aurora B mRNA, * $p<0.05$. (n=3, mean ± SEM). **(E)** Effect of Xbp1 gene silencing and p38 inhibition on uXbp1 expression in NRVM. *** $p<0.001$. (n=3, mean ± SEM). (**F**) Effect of Xbp1

gene silencing and p38 inhibition on cardiomyocyte proliferation based on Ki67 and Aurora B mRNA, * $p<0.05$. (n=3, mean ± SEM). (**G**) Cell-cycle regulatory genes as candidate downstream targets of Xbp1 and differentially expressed in the p38cdKO RV at P3. p value and FC are calculated from RNAseq results. (**H**) Cell surface area of NRVMs treated with p38 inhibitor or IRE1α overexpression. (3 independent experiments.) (**I**) Cell surface area of NRVMs transfected with siXbp1 or control. (3 independent experiments.)

SUPPLEMENTAL TABLES

Table S1. Survival of p38 cdKO mouse.

Table S2. List of differentially expressed genes in P1 p38cdKO RV vs. Control

Table S3. List of differentially expressed genes in P3 p38cdKO RV vs. Control

Table S4. List of differentially expressed genes in P1 p38cdKO LV vs. Control

Table S5. List of differentially expressed genes in P3 p38cdKO LV vs. Control.

Table S6. List of differentially expressed genes between RV and LV in P3 Control mice.

Table S7. Primer sequences used for qRT-PCR.

Table S8. List of antibodies and their sources used in this study.

SUPPLEMENTAL MOVIE FILES

Supplemental Movie 1, 2. Representative images of 3D reconstruction of P3 Control heart recorded by light-sheet microscopy.

Supplemental Movie 3, 4. Representative images of 3D reconstruction of P3 p38cdKO heart recorded by light-sheet microscopy.

SUPPLEMENTAL EXPERIMENTAL PROCEDURES

Cells

Neonatal rat ventricular myocytes (NRVM) were prepared from 2 day old Sprague Dawley rat by enzymatic digestion with collagenase (Worthington) and pancreatin (Sgima) in 1xADS buffer at 37ºC as described previously [1]. NRVM were cultured in serum-free DMEM supplemented with 100U/mL Pen/Strep (Invitrogen) and 1% ITS (w/v) (BD Biosciences).

Masson-Trichrome Staining

Heart histology slides were rehydrated and stained using masson-trichrome staining kit (Sigma-Aldrich) in accordance with the manufacturer's instructions. Fibrosis was visualized under microscope under bright field.

Immunohistochemistry

Dissected mouse hearts were fixed in 10% paraformaldehyde (PFA) and embed in paraffin. These hearts were sectioned in 5um-tickness. The following antibodies were used for staining at indicated dilutions; anti-tropomyosin (1:200) (T9283, Sigma Aldrich); ki67 (1:200) (ab15580, Abcam); phosho-Histone H3 (Ser10) (06-570,

Millipore). Nuclei were stained with Hoechst 33342 (H3570, Life technologies). Secondary antibodies were obtained from Life Technologies. TUNEL staining were conducted using In situ Cell Death Detection Kit (Roche) in accordance with the manufacturer's instructions. WGA staining was conducted using Alexa Fluor 594 conjugated WGA reagent (1:200) (Life technologies) in accordance with the manufacturer's instructions.

For pH3/TPM, TUNEL/TPM, and WGA staining, 2-4images (depends on the wall size) were taken to cover the most of ventricular free wall with x20 magnification for analyzing. pH3 or TUNEL positive myocyte nuclei and myocyte nuclei were counted using Nikon software. For WGA staining, cross-sectional area was analyzed using Nikon software. To calculate total number of myocyte nuclei in whole LV or RV free-wall, number of myocyte nuclei per area and total area of each ventricle free-wall were measured.

RNA and protein extraction

Dissected hearts were separated in four chambers. Only free-wall of the RV and

LV were used for RNA or protein extraction. Total RNA was extracted from tissue or cultured NRVMs using TRIzol reagent (Life technologies) in accordance with the manufacturer's instructions. Nuclear and cytoplasmic RNA were extracted using Cytoplasmic & Nuclear RNA Purification Kit (Noren Biotek) in accordance with the manufacturer's instructions.

Real-time PCR

1μg RNA was used for first-strand cDNA synthesis using Random Primer (Invitrogen) and SuperScriptII Reverse Transcriptase (Invitrogen) in accordance with the manufacturer's instruction. Real-time PCR was performed using IQ SYBR Green Supermix (Bio-Rad) with CFX-96 Real-time PCR Detection System (Bio-Rad) as previously described [2]. Primer sequence are listed in **Table S7**.

Semi-quantitative PCR

cDNA from cell lysate were used for PCR reaction. PCR reaction was performed using 2x Taq PCR Premix (Bioland Scientific LLC). Primers are listed in Table S7. PCR products were loaded onto 4-5% agarose gel containing GelRed Nucleic Acid Gell Stain (Biotiun). Images of the gel was acquired with a high resolution CCD camera (ChemiDoc

XRS^{+} Bio-Rad) and quantification of the bands was performed by Image Lab (Bio-Rad).

RNAseq data analysis

A total of 1μg RNA per sample was processed via poly-A selection and fragmentation. The first-strand cDNA was generated using random primer based reverse transcription and subsequently used for generating second-strand cDNA using RNase H and DNA polymerase. Sequence adapters were ligated using the Illumina Paired-End sample prep kit. Fragments of ~200bp were isolated by gel electrophoresis, amplified by 15 cycles of PCR and sequenced on the Illumina Genome Analyzer II in the paired-end sequencing protocol as described[3]. RNA-sequencing Raw reads were trimmed for adapters and analyzed using FASTQC, read fragments with quality <28 were removed. Samples were then mapped to the mm10 genome using bowtie2 and analyzed using cufflinks. Principal Component Analysis (PCA) was generated using ggbiplot on all expressed genes defined as > 0.5 FPKM. Differential expression was calculated using CuffDiff with standard parameters. The data was cut-offed based on Fold change>1.2 and $p<0.05$. Differentially expressed gene lists (control vs. cdKO) were identified using DAVID Bioinformatics Resources 6.8 (https://david.ncifcrf.gov) to obtain GO

classification results. These differentially expressed lists were also submitted to whole-Genome rVISTA (http://genome.lbl.gov/vista/index.shtml) to determine the names and the number of over-represented and conserved transcriptional factor binding sit in 5000 bp upstream of the differentially-expressed genes.

Immunoblot

The concentrations of protein lysates were measured using BCA protein assay reagent (Thermo Scientific) in accordance with the manufacturer's instructions. 50 ug of total proteins were used for sample preparation. Targeted proteins were detected as previously described [1]. Antibodies against phosphor-p38, p38, phosphor-JNK, JNK, phosphor-ERK1/2, ERK1/2, phosphor-Histone H3, Histone H3, phosphor-Akt, Akt, Gsk3b, cleaved Caspase3, PCNA, BIRC5, p21 were purchased from Cell Signaling. Antibodies against CyclinD1, Bax, Bcl2, phosphor-Bad, Bad, Actin, GAPDH were purchased from Santa Cruz. Antibodies against phosphor-Rb, Rb, Wee1, Cdk1 were purchased from Abcom. Antibody against Bcl2l11 was purchased from Sigma Aldrich. The antibodies and their usage were listed in Supplemental **Table S8**. Images of the gel was acquired with a high-resolution CCD camera (ChemiDoc XRS$^+$ Bio-Rad) and

quantification of the bands was performed by Image Lab (Bio-Rad).

Embryo Clarity Method

The mouse hearts were infused with acrylamide monomer solution overnight at 4 degrees C. Acrylamide monomer solution was formulated with 4% acrylamide (Bio-Rad) and 0.5% w/v of the photoinitiator 2,2'-Azobis[2-(2-imidazolin-2-yl)propane]dihydrochloride (VA-044, Wako Chemicals USA), in a 1x phosphate buffered saline (PBS) solution. The heart samples were subsequently incubated at 37 degrees C for 2-3 hours to initiate polymerization of the acrylamide into a polyacrylamide gel matrix. Afterwards, the samples were rinsed in 1x PBS and placed in a clearing solution that consisted of 8% w/v sodium dodecyl sulfate (SDS, Sigma Aldrich) and 1.25% w/v boric acid (Fisher) with a final solution pH of 8.4. The mouse hearts were incubated at 37 degrees in clearing solution for 4 weeks with periodic replacement of fresh clearing solution every 36 hours. Once the samples were cleared, the tissues were rinsed over 24 hours with 1x PBS to remove residual SDS solution. To prepare the samples for imaging, the cleared mouse hearts were incubated with refractive index matching solution (RIMS) at room temperature for 24 hours. To make RIMS, we dissolved 40 grams of Histodenz

(Sigma) in 30 mL of 0.02M Phosphate buffer (Sigma). 0.05% w/v of sodium azide (Sigma) was added as a preservative for the RIMS solution. The RIMS solution was then sterile filtered and stored at room temperature until use.

Light-sheet microscopic imaging

Light sheet imaging was carried out on a home-made system. A diode-pumped solid-state laser (LMM-GB1, Laserglow Technologies, Toronto, Canada) was used as the 532 nm illumination source. The initial diameter of laser beam was 2 mm, and then light passed through a 5x achromatic beam expander (GBE05-A, Thorlabs Inc, New Jersey, USA). A beam splitter (BS013, Thorlabs Inc, New Jersey, USA) was employed to form dual-illumination onto the sample from opposite directions. Each beam was focused by a plano-convex cylindrical lens (f=50 mm, LJ1695RM-A, Thorlabs Inc, New Jersey, USA) and was then reshaped by a group of achromatic doublets (AC254-060-A, AC254-100-A, Thorlabs, New Jersey, USA). After passing through an f=150 mm lens, the beam expanded to a sheet with the width of 40 mm, as well as the waist of 17 μm. The detection module was installed perpendicular to the illumination plane, and it was composed of a stereo microscope (MVX10, Olympus, Japan) with a 1x magnification objective

(Numerical aperture, NA: 0.25), a scientific CMOS (ORCA-Flash4.0LT, Hamamatsu, Japan) and optical filters (Semrock, New York, USA). The sample with RIMS and 1% agarose solution was embedded in a Borosilicate glass tubing whose inner diameter was less than 6 mm, and then the mounted sample was held to be oriented and moved by a motorized translational stage. Both the sample and its holder except for the translational stage were immersed in a transparent chamber which was full of 99.5% glycerol to match the refractive index among different materials. Illumination and detection are controlled by a computer with dedicated SSD RAID 0 storage for fast data streaming.

REFERENCES IN SUPPLEMENTAL MATERIAL

1. Ota A, Zhang J, Ping P, Han J and Wang Y. Specific regulation of noncanonical p38alpha activation by Hsp90-Cdc37 chaperone complex in cardiomyocyte. *Circ Res*. 2010;106:1404-12.

2. Gao C, Ren S, Lee JH, Qiu J, Chapski DJ, Rau CD, Zhou Y, Abdellatif M, Nakano A, Vondriska TM, Xiao X, Fu XD, Chen JN and Wang Y. RBFox1-mediated RNA splicing regulates cardiac hypertrophy and heart failure. *J Clin Invest*. 2016;126:195-206.

3. Lee JH, Gao C, Peng G, Greer C, Ren S, Wang Y and Xiao X. Analysis of transcriptome complexity through RNA sequencing in normal and failing murine hearts. *Circ Res*. 2011;109:1332-41.

FigS1

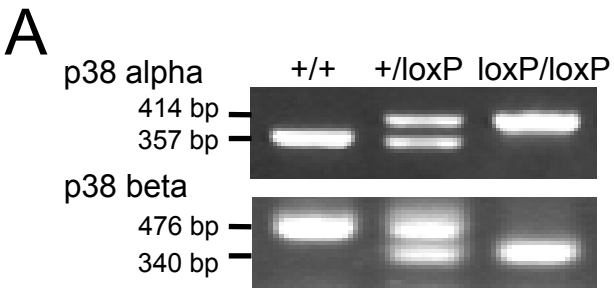
A
p38 alpha
+/+
+/loxP
loxP/loxP
414 bp
357 bp
p38 beta
476 bp
340 bp

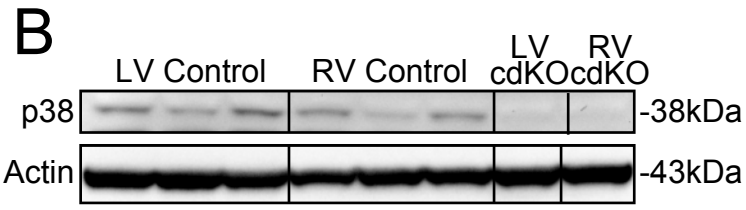
B
LV Control
RV Control
LV cdKO
RV cdKO
p38
-38kDa
Actin
-43kDa

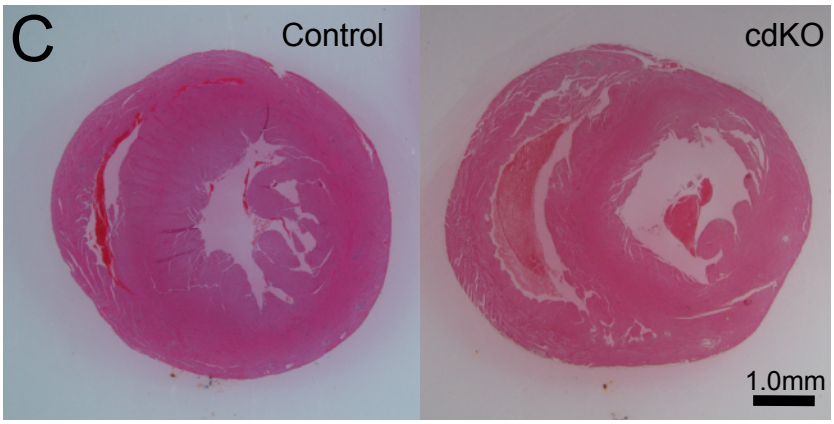
C
Control
cdKO
1.0mm

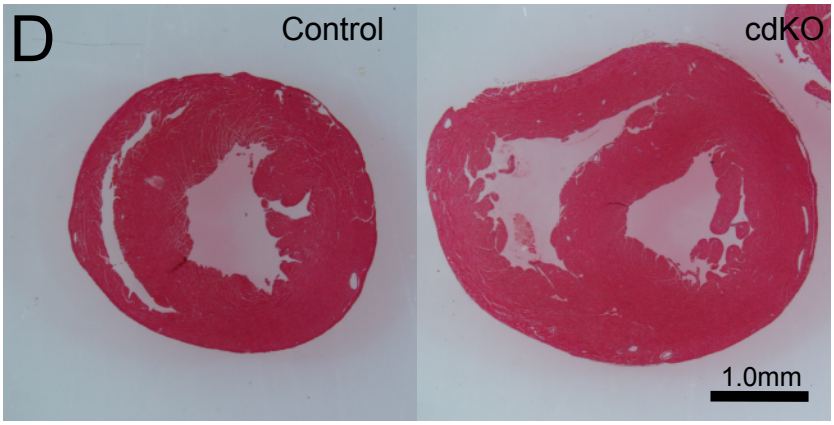
D
Control
cdKO
1.0mm

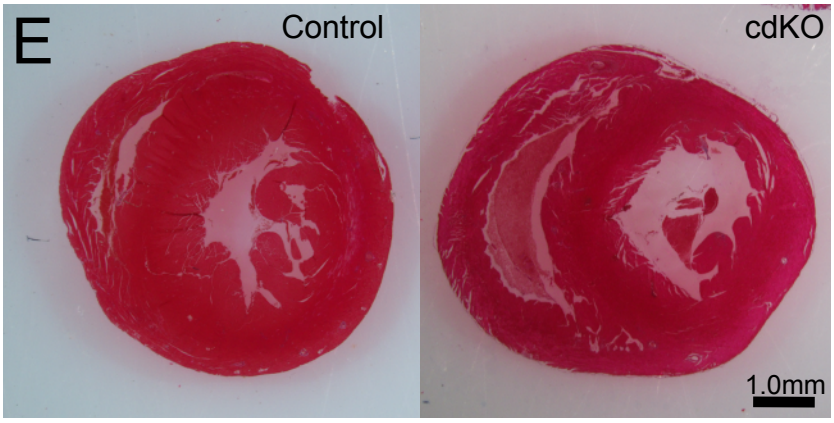
E
Control
cdKO
1.0mm

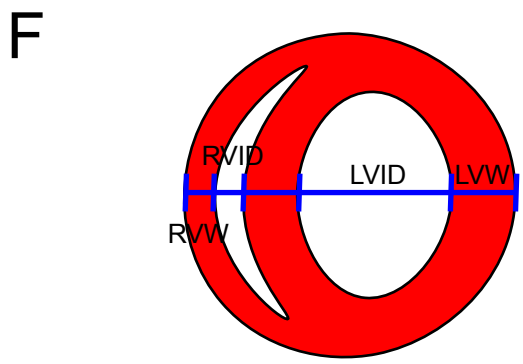
F
RVID
LVID
LVW
RVW

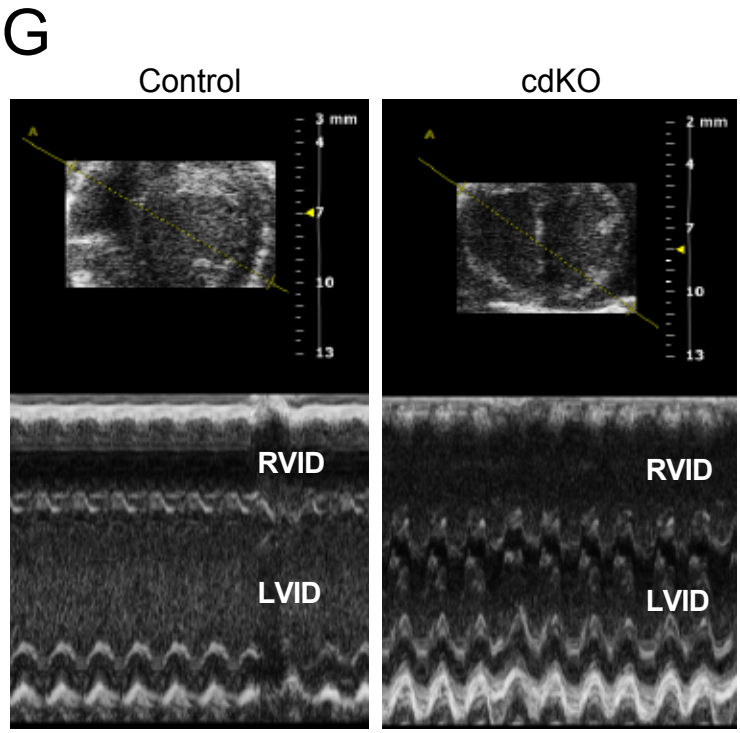
G
Control
cdKO
RVID
LVID
RVID
LVID

FigS2

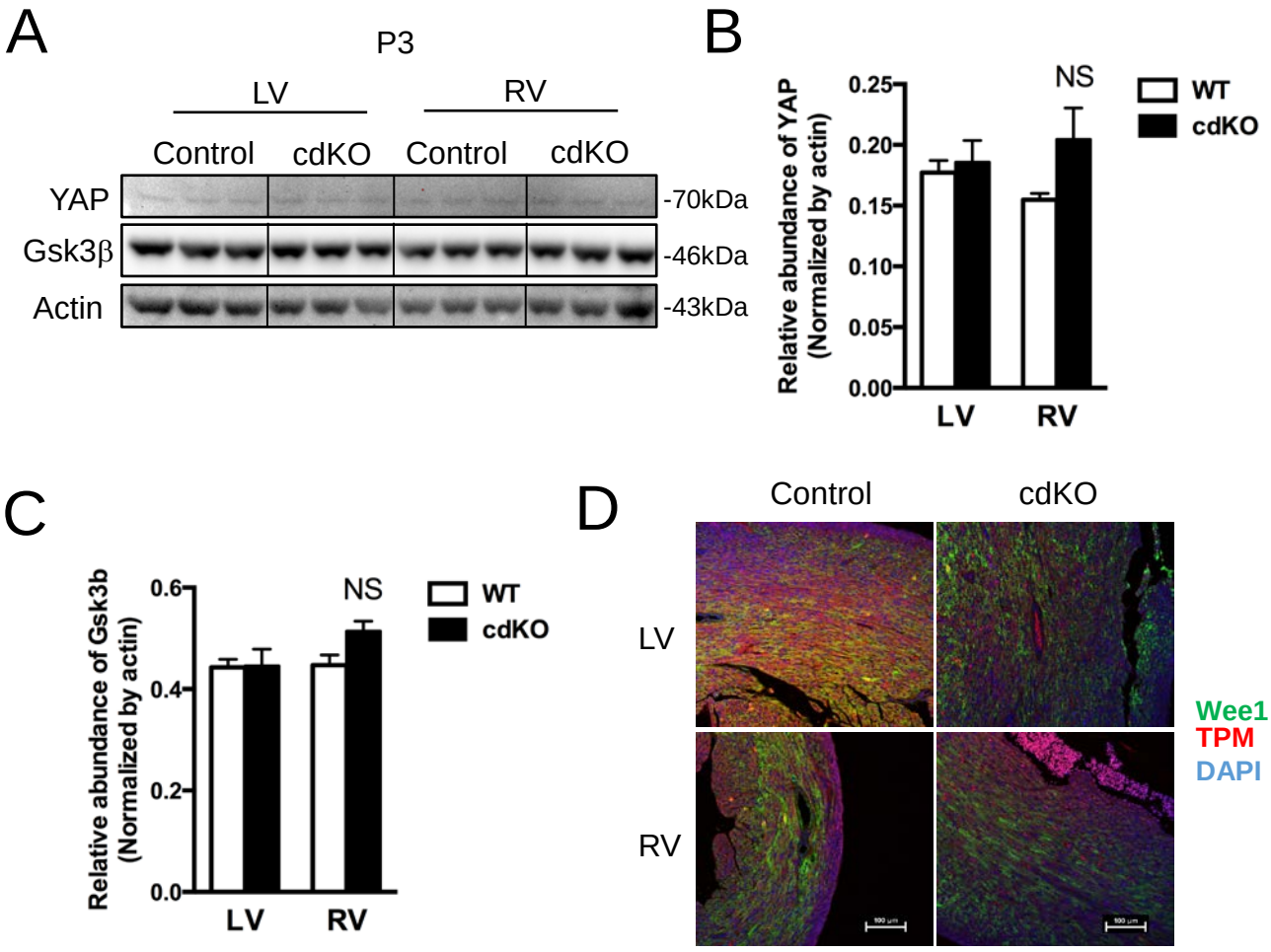
A
P3
LV
RV
Control
cdKO
Control
cdKO
YAP
Gsk3β
Actin
-70kDa
-46kDa
-43kDa
B
Relative abundance of YAP (Normalized by actin)
0.25
0.20
0.15
0.10
0.05
0.00
NS
WT
cdKO
LV
RV
C
Relative abundance of Gsk3b (Normalized by actin)
0.6
0.4
0.2
0.0
NS
WT
cdKO
LV
RV
D
Control
cdKO
LV
RV
Wee1
TPM
DAPI

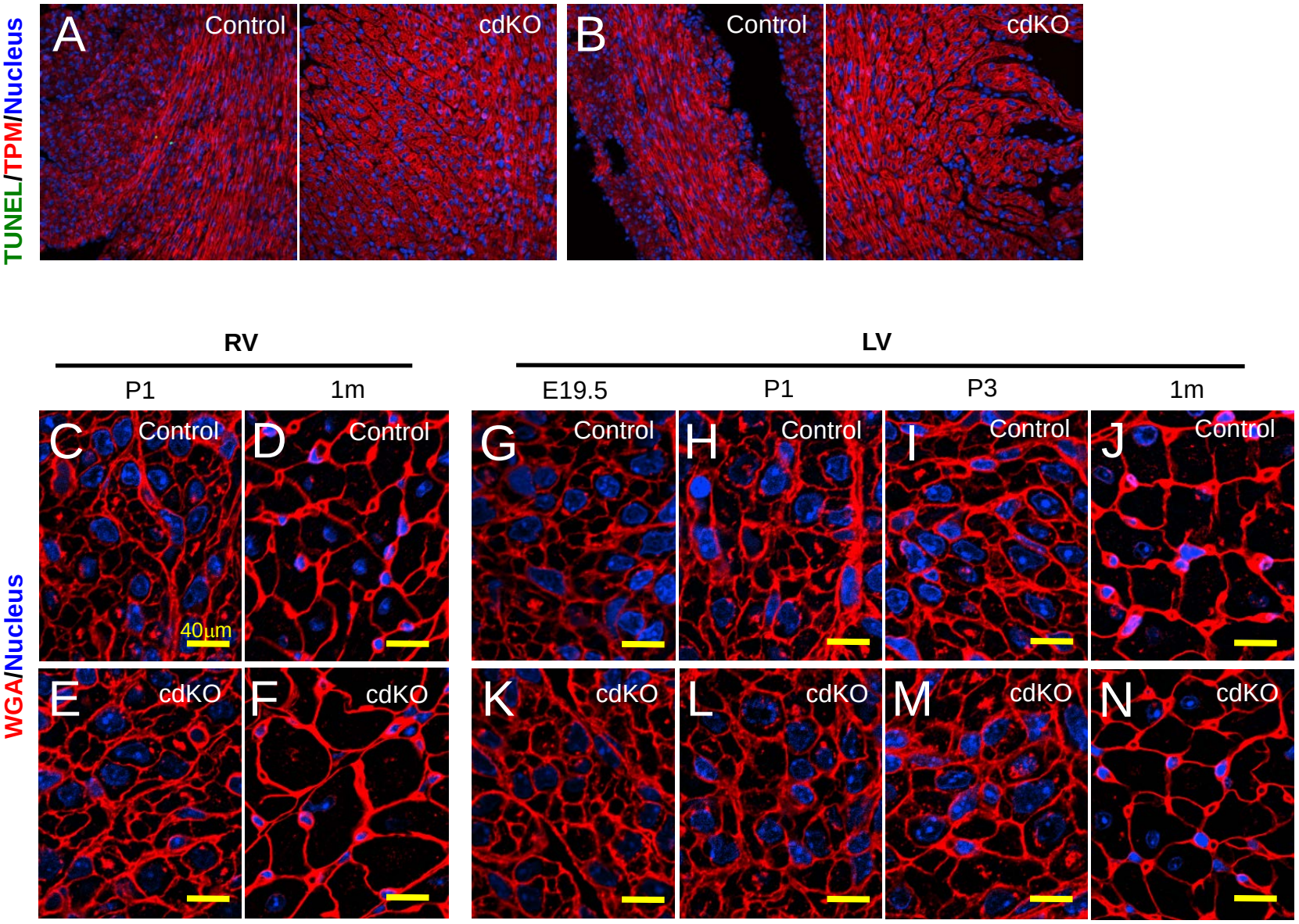
TUNEL/TPM/Nucleus
A
Control
cdKO
B
Control
cdKO
RV
LV
P1
1m
E19.5
P1
P3
1m
C
Control
D
Control
G
Control
H
Control
I
Control
J
Control
40μm
WGA/Nucleus
E
cdKO
F
cdKO
K
cdKO
L
cdKO
M
cdKO
N
cdKO

FigS4

A

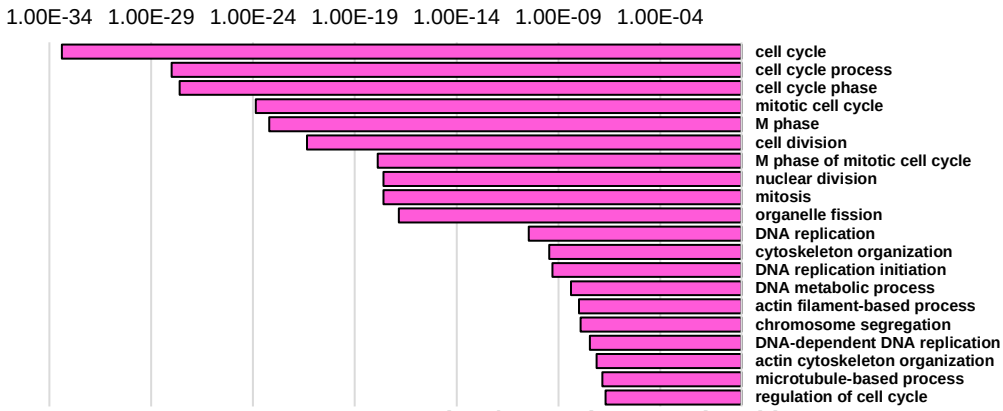
cdKO/Control up-regulated in LV at P1
1.00E-34
1.00E-29
1.00E-24
1.00E-19
1.00E-14
1.00E-09
1.00E-04
cell cycle
cell cycle process
cell cycle phase
mitotic cell cycle
M phase
cell division
M phase of mitotic cell cycle
nuclear division
mitosis
organelle fission
DNA replication
cytoskeleton organization
DNA replication initiation
DNA metabolic process
actin filament-based process
chromosome segregation
DNA-dependent DNA replication
actin cytoskeleton organization
microtubule-based process
regulation of cell cycle

B

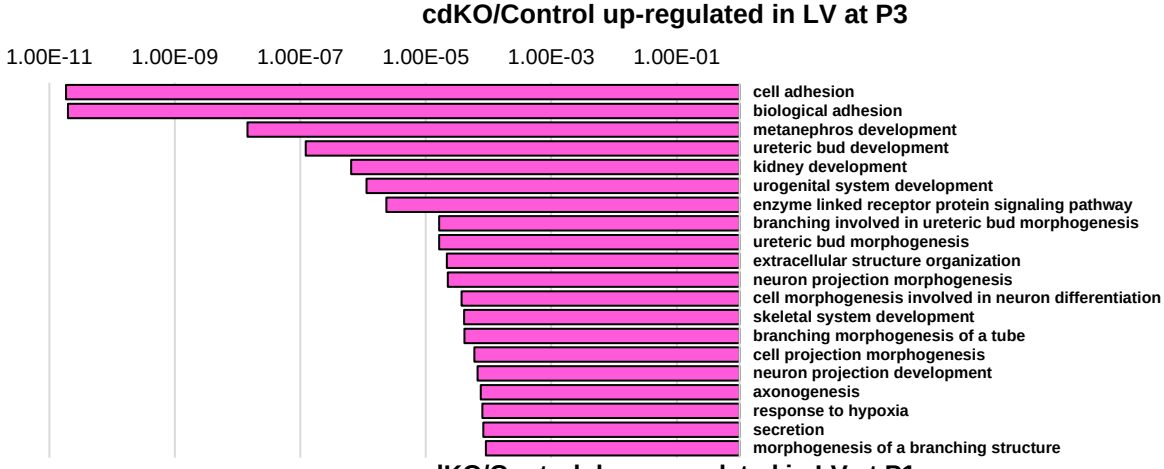
cdKO/Control up-regulated in LV at P3
1.00E-11
1.00E-09
1.00E-07
1.00E-05
1.00E-03
1.00E-01
cell adhesion
biological adhesion
metanephros development
ureteric bud development
kidney development
urogenital system development
enzyme linked receptor protein signaling pathway
branching involved in ureteric bud morphogenesis
ureteric bud morphogenesis
extracellular structure organization
neuron projection morphogenesis
cell morphogenesis involved in neuron differentiation
skeletal system development
branching morphogenesis of a tube
cell projection morphogenesis
neuron projection development
axonogenesis
response to hypoxia
secretion
morphogenesis of a branching structure

C

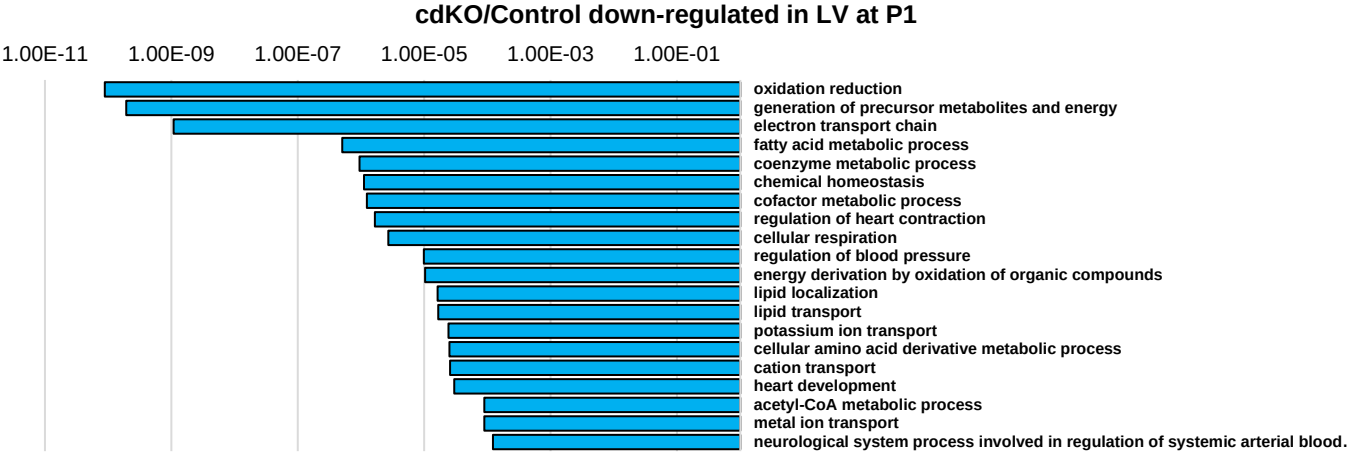
cdKO/Control down-regulated in LV at P1
1.00E-11
1.00E-09
1.00E-07
1.00E-05
1.00E-03
1.00E-01
oxidation reduction
generation of precursor metabolites and energy
electron transport chain
fatty acid metabolic process
coenzyme metabolic process
chemical homeostasis
cofactor metabolic process
regulation of heart contraction
cellular respiration
regulation of blood pressure
energy derivation by oxidation of organic compounds
lipid localization
lipid transport
potassium ion transport
cellular amino acid derivative metabolic process
cation transport
heart development
acetyl-CoA metabolic process
metal ion transport
neurological system process involved in regulation of systemic arterial blood.

D

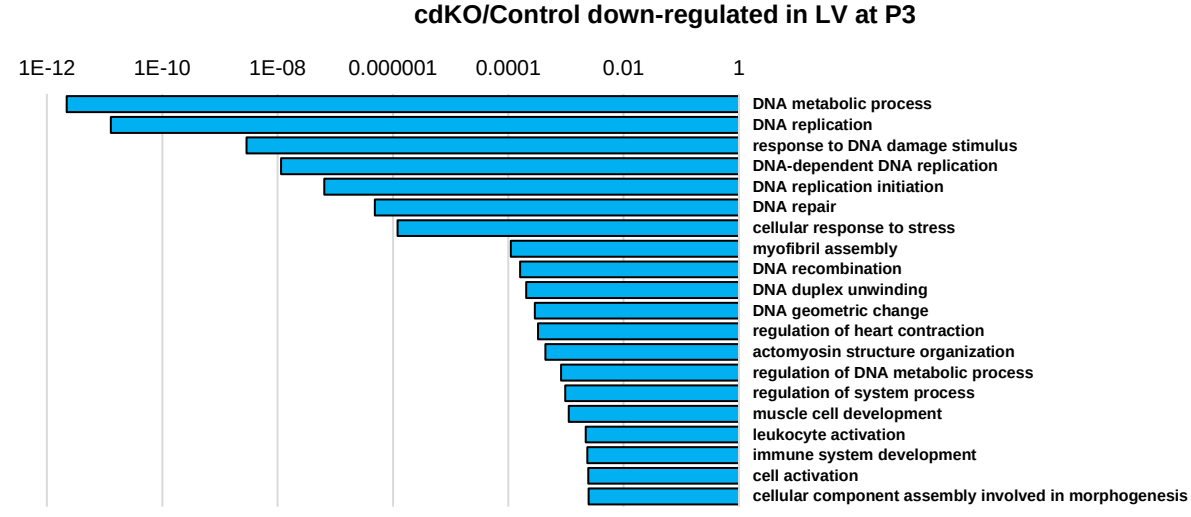
cdKO/Control down-regulated in LV at P3
1E-12
1E-10
1E-08
0.000001
0.0001
0.01
1
DNA metabolic process
DNA replication
response to DNA damage stimulus
DNA-dependent DNA replication
DNA replication initiation
DNA repair
cellular response to stress
myofibril assembly
DNA recombination
DNA duplex unwinding
DNA geometric change
regulation of heart contraction
actomyosin structure organization
regulation of DNA metabolic process
regulation of system process
muscle cell development
leukocyte activation
immune system development
cell activation
cellular component assembly involved in morphogenesis

FigS4

E

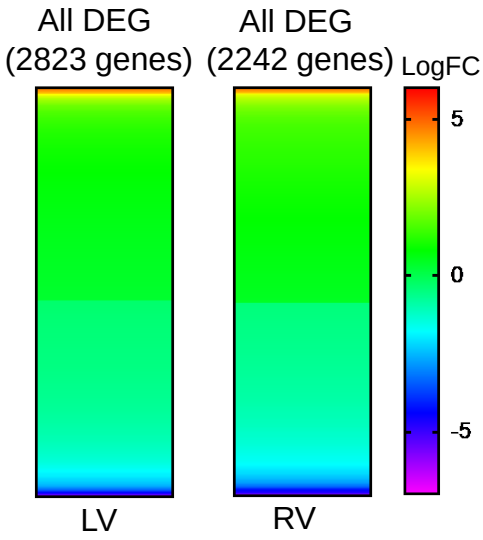
All DEG
(2823 genes)
All DEG
(2242 genes)
LogFC
5
0
-5
LV
RV

F

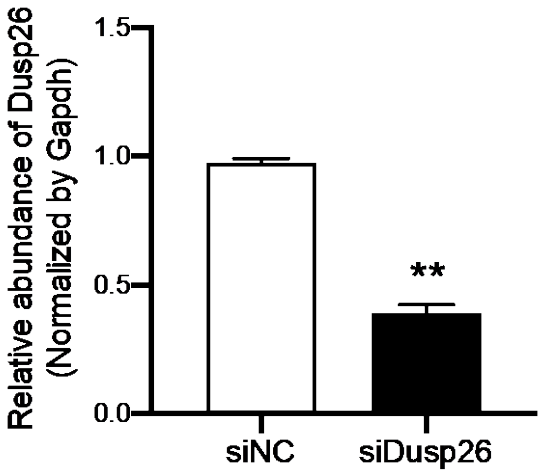
Relative abundance of Dusp26
(Normalized by Gapdh)
1.5
1.0
0.5
0.0
**
siNC
siDusp26

FigS5

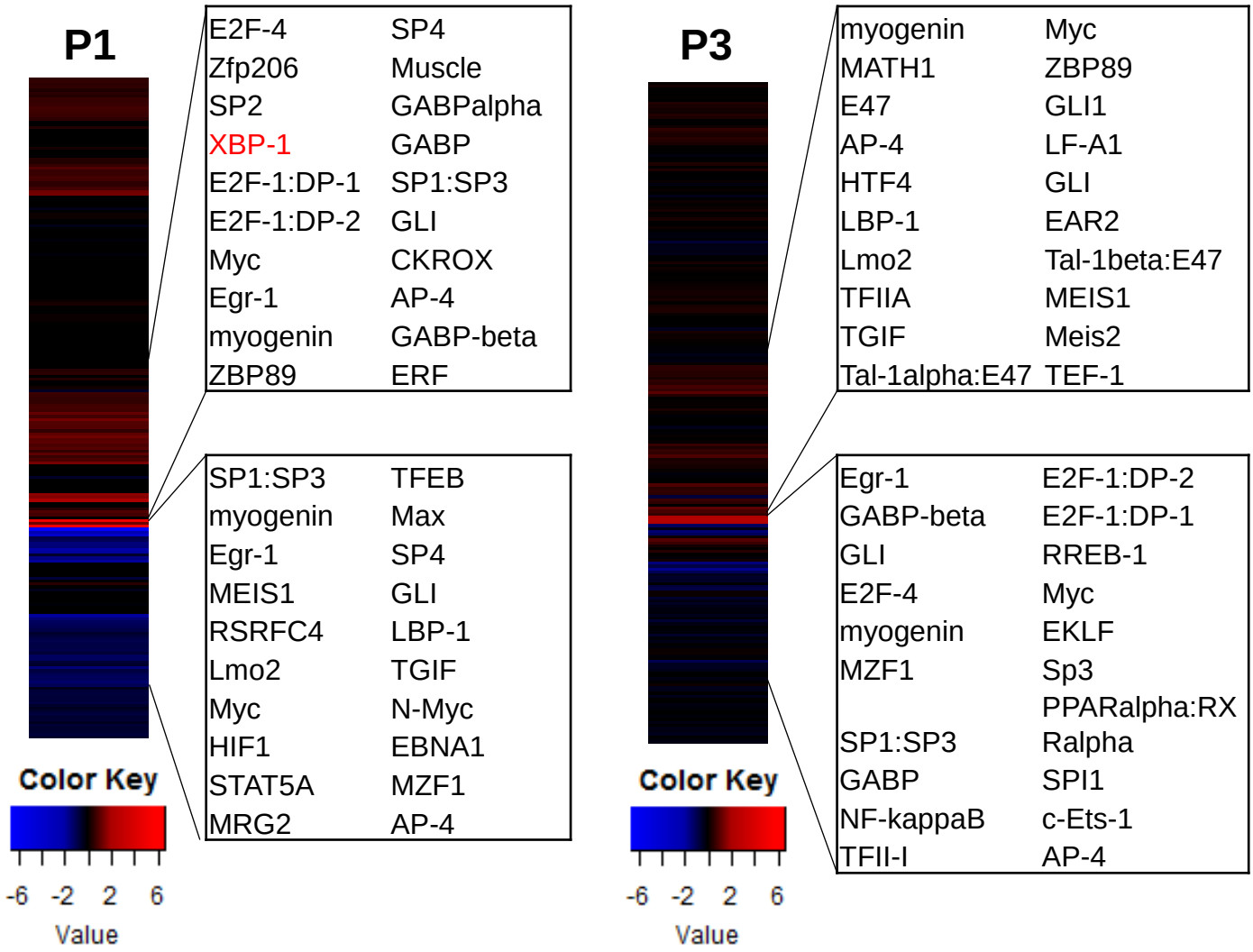
P1
E2F-4 SP4
Zfp206 Muscle
SP2 GABPalpha
XBP-1 GABP
E2F-1:DP-1 SP1:SP3
E2F-1:DP-2 GLI
Myc CKROX
Egr-1 AP-4
myogenin GABP-beta
ZBP89 ERF
SP1:SP3 TFEB
myogenin Max
Egr-1 SP4
MEIS1 GLI
RSRFC4 LBP-1
Lmo2 TGIF
Myc N-Myc
HIF1 EBNA1
STAT5A MZF1
MRG2 AP-4
Color Key
-6 -2 2 6
Value
P3
myogenin Myc
MATH1 ZBP89
E47 GLI1
AP-4 LF-A1
HTF4 GLI
LBP-1 EAR2
Lmo2 Tal-1beta:E47
TFIIA MEIS1
TGIF Meis2
Tal-1alpha:E47 TEF-1
Egr-1 E2F-1:DP-2
GABP-beta E2F-1:DP-1
GLI RREB-1
E2F-4 Myc
myogenin EKLF
MZF1 Sp3
PPARalpha:RX
SP1:SP3 Ralpha
GABP SPI1
NF-kappaB c-Ets-1
TFII-I AP-4
Color Key
-6 -2 2 6
Value

FigS6

A

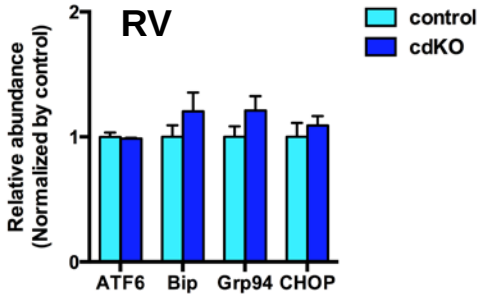

B

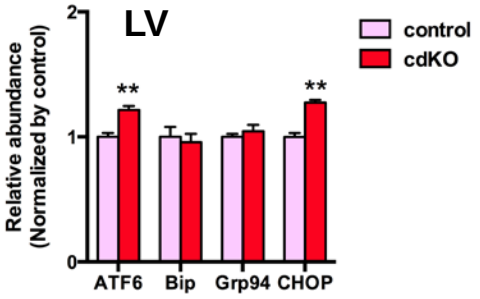

C

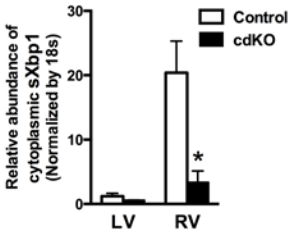

D

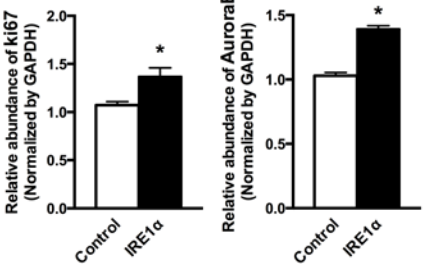

E

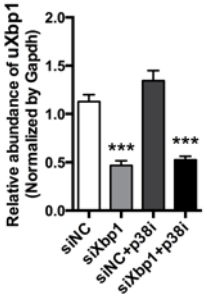

F

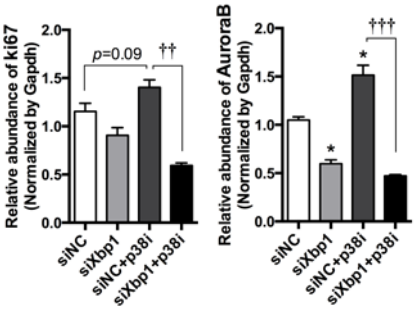

G

Gene symbol	Function	P-value	FC
Fgfr2	positive regulation of cell cycle	0.000	2.04
Lif	negative regulation of meiotic nuclear division	0.000	3.19
Fam83d	cell cycle	0.000	1.65
Bre	cell cycle	0.000	1.55
Ccnb2	cell cycle	0.000	1.51
Gas2l3	cell cycle arrest	0.001	1.46
Ctdspl	negative regulation of G1/S transition of mitotic cell cycle	0.001	1.40
Cdca3	cell cycle	0.001	1.43
Cdc20	cell cycle	0.001	1.48

H

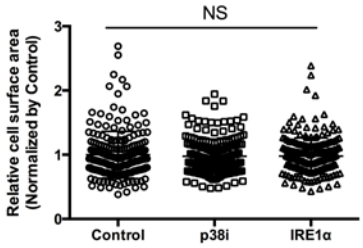

I